JOURNAL OF CONSTRUCTIONAL STEEL RESEARCH

Journal of Constructional Steel Research 57 (2001) 113–134

www.elsevier.com/locate/jcsr

Strength of short concrete filled high strength steel box columns

B. Uy *

School of Civil and Environmental Engineering, The University of New South Wales, Sydney, NSW 2052, Australia

Received 20 July 1999; received in revised form 13 March 2000; accepted 12 May 2000

Abstract

The use of concrete filled steel box columns has been consistently applied in the design of tall buildings as they provide considerable economy in comparison with conventional steel columns. Their use allows the adoption of steel or composite floor systems combined with economically constructed columns. The use of these columns also has considerable advantages over reinforced concrete columns as they allow higher percentages of reinforcement to be adopted. In basements of tall buildings where car park space is of premium cost, a reduction in the column size can provide significant economic benefits. The use of high strength steel can be applied in these situations. This paper provides an extensive set of experiments on high strength steel box columns filled with concrete. A numerical model is presented and calibrated successfully with these tests. Furthermore, comparisons with the Eurocode 4 model for composite columns are also undertaken in this paper and this is found to be unconservative in its prediction of axial and combined strength. A mixed analysis technique is therefore presented, which treats the concrete as rigid plastic and the steel as linear elastic. This model is calibrated well with the numerical model presented and both of these models are found to be conservative in predicting the test results. © 2001 Elsevier Science Ltd. All rights reserved.

Keywords: Box columns; Composite columns; High strength steel; Local buckling; Steel columns; Welded columns

* Tel.: +61-2-9385-5474; fax: +61-2-9385-6139.
E-mail address: b.uy@unsw.edu.au (B. Uy).

PII: S0143-974X(00)00014-6

Nomenclature

A	area
b	steel plate width
B	column width
d_n	neutral axis depth
D	depth of column
e	eccentricity
E	elastic modulus of steel
f_c	mean compressive strength of concrete
h_n	height of neutral axis above centroidal axis
k	local buckling coefficient
L	length of column
M	bending moment
N	axial force
N_u	ultimate axial force
t	steel plate thickness
y	lever arm
ε	strain
ν	Poisson's ratio
ρ	curvature
σ	stress
σ_{ol}	local buckling stress
σ_u	ultimate stress
σ_y	yield stress

1. Introduction

Concrete filled steel box columns have recently experienced a renaissance in their use throughout the world in multistorey building construction. This has been promulgated by their use in many significant tall buildings where savings in construction costs are of major importance to the overall project. This last decade has also seen a plethora of research undertaken into individual member behaviour, together with these columns as part of entire frameworks.

The use of high strength structural steel has generally been limited in most nations, however it has been shown to be able to provide significant savings through the increase in floor areas which column members can provide. Recent research has also shown that high strength structural steel can be designed according to existing structural steel standards, particularly if local buckling slenderness limits are adhered to [1, 2]. Furthermore, Uy and Sloane [3] have shown that the local buckling slenderness limits for high strength structural steel can be relaxed when the steel is restrained by concrete from local buckling as is the case in composite beams in positive bending. Uy [4] also illustrated an increase in local buckling slenderness limits for mild structural steel box columns filled with concrete in an extensive experimental and numerical study.

High strength fabricated steel columns may be more economical than traditional steel sections when the axial load demand on columns increases the cross-sectional size. Design applications have arisen in tall buildings in Australia and Japan where the use of high strength structural steel was more economical than the use of mild structural steel, because column dimensions were reduced and floor area was increased thus providing significant cost savings [5].

This paper presents an extensive set of experiments on the behaviour of concrete filled high strength steel box columns as illustrated in Fig. 1, which were fabricated using four steel plates of equal length and thickness and fillet welded at their edges. These experiments are used to calibrate a numerical model developed elsewhere. Both the model and the experiments are then compared with the current approach adopted in Eurocode 4 [6]. This paper will show that whilst the numerical model is conservative, the Eurocode 4 model needs modifications in order to provide a conservative result in estimating the member cross-sectional strength. A mixed analysis approach is therefore suggested which is found to provide a conservative estimate of the cross-sectional strength under combined bending and compression and is thus amenable for design.

2. Experiments

This section outlines three series of experiments undertaken to determine the combined behaviour under compression and bending for high strength steel box columns filled with concrete.

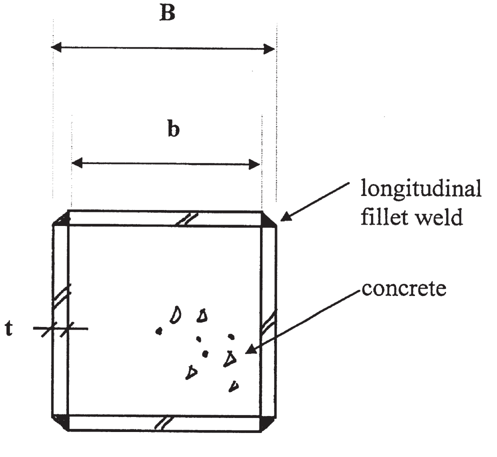

Fig. 1. Concrete filled steel column cross-section.

2.1. Test series

Three series of tests were undertaken and these are summarised in Table 1. Each series had a different plate slenderness limit, however all were considered to be compact in terms of restrained local buckling slenderness limits and thus no reduction due to local buckling of the component plates was expected. The local buckling slenderness limits for high strength structural steel can be determined by using the local buckling coefficients derived by Uy and Bradford [7], where the local buckling stress is determined from Eq. (1)

$$\sigma_{\mathrm{ol}}=\frac{k\pi^2E}{12(1-\nu^2)\left(\frac{b}{t}\right)^2} \tag{1}$$

Now the local buckling coefficient was taken to be k=10.31 as determined by Uy and Bradford [7] in their study of local buckling of plates in composite members. The elastic modulus was taken as E=200,000 MPa, and the Poisson's ratio ν=0.30. If the nominal yield stress is taken as 690 MPa, the yield slenderness limit is therefore calculated using Eq. (2), where

$$\frac{b}{t}=\sqrt{\frac{k\pi^2E}{12(1-\nu^2)\sigma_{\mathrm{y}}}}=\sqrt{\frac{10.31\times\pi^2\times200{,}000}{12\times(1-0.30^2)\times690}}=52 \tag{2}$$

Each of the series had a slenderness limit lower than this and thus the component plates were considered as compact as highlighted in Table 1. However it should be pointed out that the yield slenderness limit for the third series of columns is in excess of that derived for hollow columns. The slenderness limit for hollow columns is 32, which can be determined by using a local buckling coefficient of 4 in Eq. (2).

2.2. Material properties

2.2.1. Steel

To ascertain the stress–strain behaviour of the steel in both tension and compression, a series of tensile coupon and stub column tests were conducted. The results of the tensile coupon tests are summarised in Table 2 and those for the stub column tests are summarised in Table 3. Typical stress–strain curves for these tests are also illustrated in Figs. 2 and 3, respectively. Furthermore, residual stress measurements were undertaken using a combination of both electric strain gauges and mechanical strain gauges across the width of the component plates. From these tests an idealised stress distribution was established and is shown in Fig. 4. Typical values for residual stresses were only 5–10% of the yield stress value as summarised in Table 4. This does, however, represent residual compressive stresses of between 35 and 70 MPa which can be quite significant when considering elastic local buckling, which would not occur in the test specimens used in this study.

Table 1
Experimental series

Specimen name	Width B (mm)	Thickness t (mm)	b/t	f_c (MPa)	σ_y (MPa)	N_u (kN)	M_u (kNm)	e (mm)	Test type comments
HSSH1	110	5	20	0	750	1644	0	0	Hollow column — axial
HSSH2	110	5	20	0	750	1561	0	0	Hollow column — axial
HSS1	110	5	20	28	750	1836	0	0	Composite column — axial
HSS2	110	5	20	28	750	1832	0	0	Composite column — axial
HSS3	110	5	20	30	750	1555	23.3	15	Composite column — axial
HSS4	110	5	20	30	750	1281	38.4	30	Composite column — axial
HSS5	110	5	20	30	750	1585	0	0	Local buckling — axial
HSS6	110	5	20	30	750	0	66	NA	Composite column — beam
HSS7	160	5	30	30	750	1308	52.3	40	Composite column — axial
HSS8	160	5	30	30	750	2868	0	0	Composite column — axial
HSS9	160	5	30	30	750	2922	0	0	Composite column — axial
HSS10	160	5	30	30	750	2024	50.6	25	Composite column — axial
HSS11	160	5	30	30	750	1979	99.0	50	Composite column — axial
HSS12	160	5	30	30	750	2242	0	0	Local buckling — axial
HSS13	160	5	30	30	750	0	141	NA	Composite column — beam
HSS14	210	5	40	32	750	3710	0	0	Composite column — axial
HSS15	210	5	40	32	750	3483	0	0	Composite column — axial
HSS16	210	5	40	32	750	3106	77.7	25	Composite column — axial
HSS17	210	5	40	32	750	2617	130.9	50	Composite column — axial
HSS18	210	5	40	32	750	2520	0	0	Local buckling — axial
HSS19	210	5	40	32	750	0	228	NA	Comosite column — beam

Table 2
Steel coupon tensile tests

Specimen number	Yield stress, σ_y (MPa)	Ultimate stress σ_u (MPa)
1	765.3	809.7
2	781.3	816.8
3	796.4	808.9
4	793.7	830.9
Mean	784.2	816.6
Standard deviation	14.2	10.2

Table 3
Steel stub column compression tests

Specimen number	Yield stress, σ_y (MPa)	Ultimate stress, σ_u (MPa)
1	757.3	833.0
2	757.3	839.1
3	750.0	779.0
Mean	754.9	817.0
Standard deviation	4.2	33.1

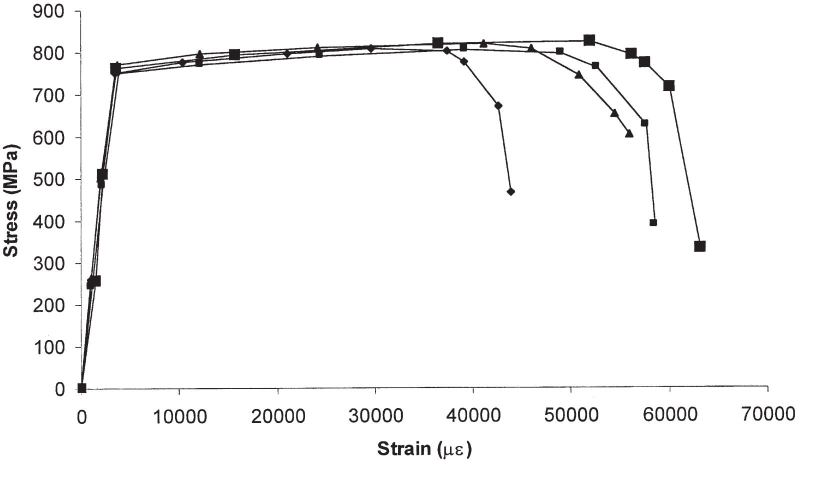

Fig. 2. Stress–strain curves for high strength structural steel in tension.

2.2.2. Concrete

In order to determine the mean compressive strength of the concrete a series of standard cylinders were crushed throughout the testing period. The results for these tests are summarised in Table 5 and the mean compressive strengths are also given for different ages of testing. This was necessary as each series was tested at a different age after casting.

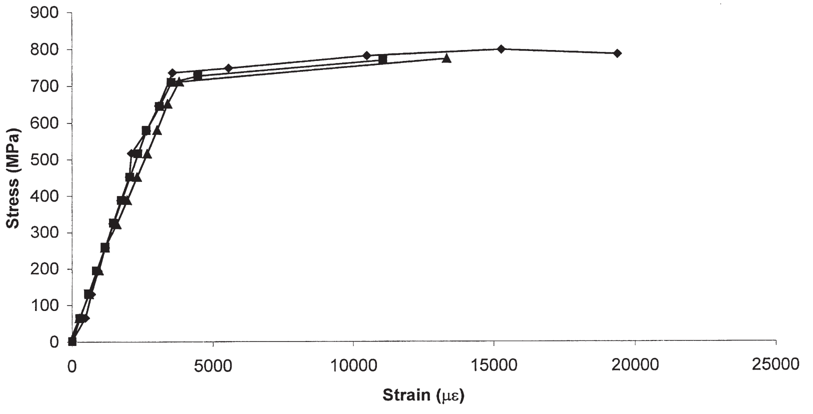

Fig. 3. Stress–strain curve for high strength structural steel in compression.

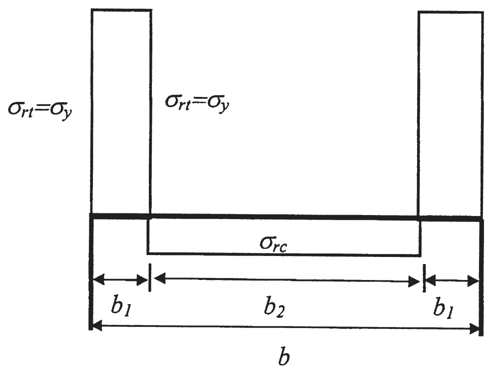

Fig. 4. Idealised residual stress distributions.

Table 4
Residual stress values

b/t	σ_r/σ_y
20	0.10
30	0.05
40	0.05

2.3. Experimental set up

2.3.1. Columns

Columns were tested in both pure compression and under combined bending and compression. In order to ensure a uniform loading surface, columns were cast in plates with plaster at either end. The eccentrically loaded columns were loaded using

Table 5
Concrete cylinder tests

Specimen number	t (days)	$f_{c(t)}$ (MPa)	$f_{c(t).average}$ (MPa)
1	28	27.4	28.7
2	28	30.0	
3	36	29.4	28.6
4	36	27.7	
5	52	30.0	30.3
6	52	30.5	
7	54	31.3	31.0
8	54	30.7	
9	55	30.8	31.4
10	55	32.0	
11	82	32.3	32.3
12	82	32.4	
13	88	32.5	32.5
14	93	32.7	32.7
15	93	32.8	

a knife-edge at both the top and bottom of the column. The test set-up including strain gauge and LVDT locations is illustrated in Fig. 5.

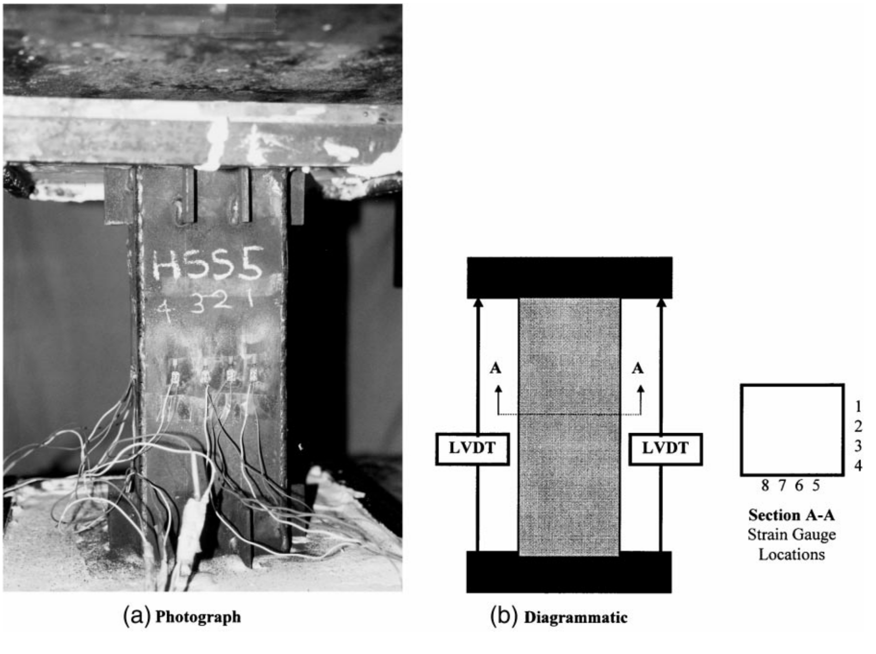

Fig. 5. Testing procedure of axially loaded columns.

2.3.2. Beams

Beams were tested in order to determine the pure flexural strength of the column cross-sections. A four point bending test was used and this provided a beam in pure bending, with the presence of shear. The test set-ups highlighting strain gauge and LVDT locations are illustrated in Fig. 6.

3. Results

This section outlines the results for failure loads and discusses pertinent failure modes of each of the specimens. For column specimens, load–axial shortening measurements were all recorded.

3.1. Failure loads

The maximum loads attained by all specimens are summarised in Table 1, where the maximum applied axial force is denoted by N_u. For the columns subjected to combined bending and compression, the maximum moment was taken as the maximum axial load N_u, multiplied by the eccentricity e. The lateral deformation of these columns was insignificant in comparison to the applied eccentricity and thus did not contribute any secondary moments. The beams tested in pure bending attained a maximum moment of M_u and this was determined as half of the peak load applied through the jack multiplied by the length of the shear span.

3.2. Load–axial shortening

Load–axial shortening measurements for each series are presented in Fig. 7. Maximum loads were obtained from these curves for specimens under pure compression. Furthermore, as the eccentricity was increased the maximum axial load able to be achieved was reduced and this was the expected result for a column under combined actions.

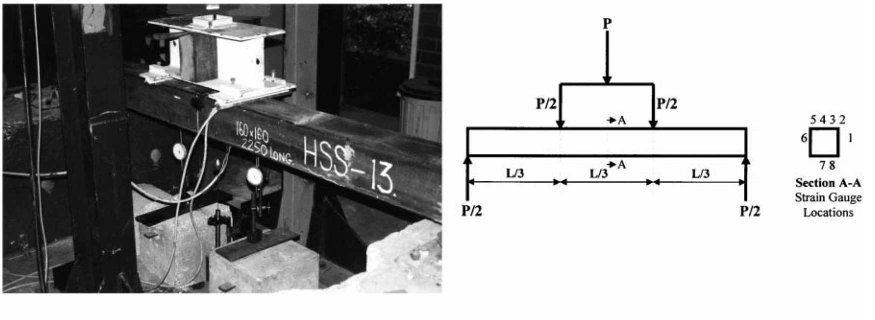

(a) Photograph (b) Diagrammatic

Fig. 6. Testing procedure of beams.

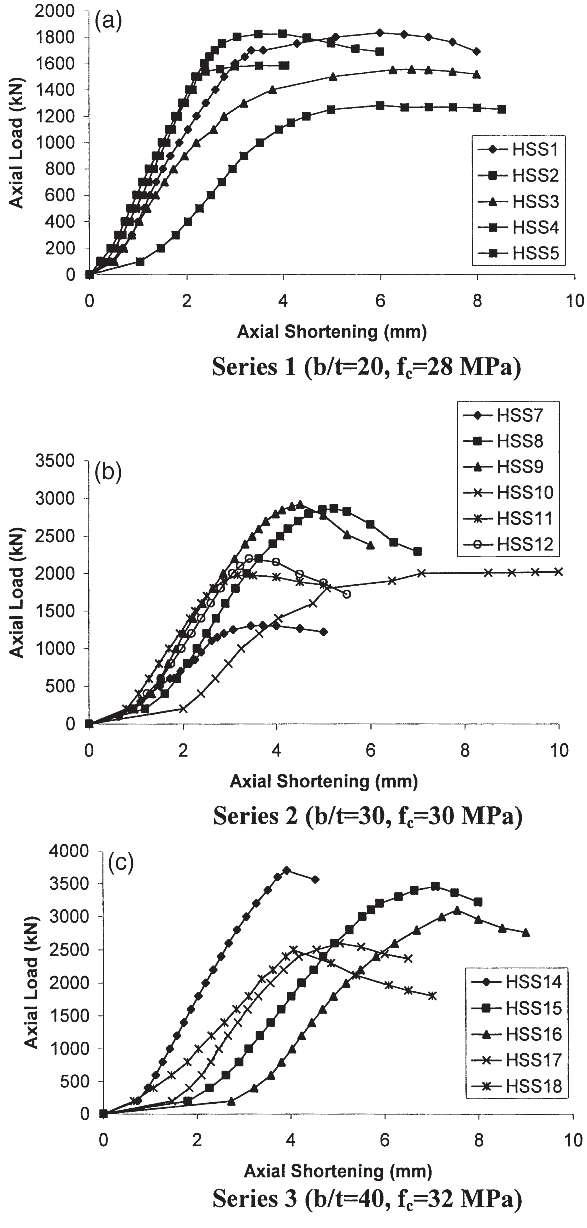

Fig. 7. Axial load–shortening curves of series 1–3.

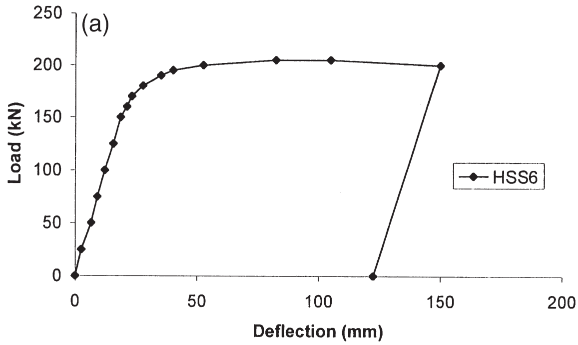

Series 1 (b/t=20, f_c=28 MPa)

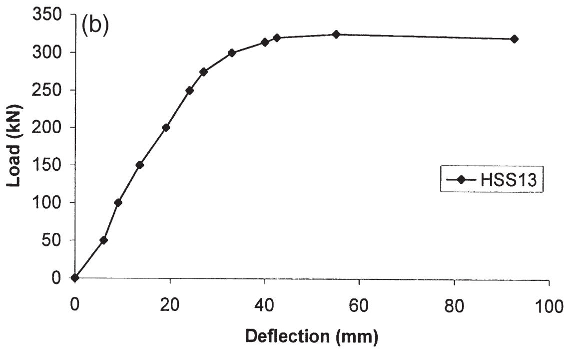

Series 2 (b/t=30, f_c=30 MPa)

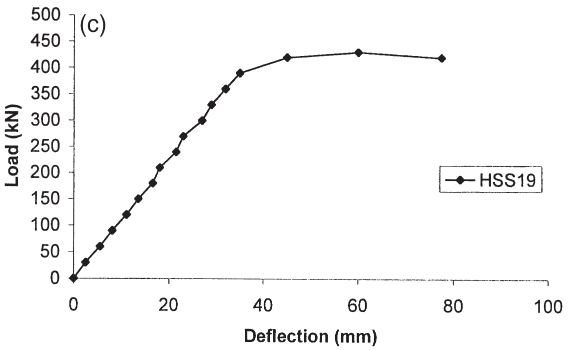

Series 3 (b/t=40, f_c=32 MPa)

Fig. 8. Load–deflection curves of beams of series 1–3.

The curves in Fig. 7 also highlight the ductile nature of failure of all the columns tested. Once the peak load was reached which was generally characterised by concrete crushing on the compressive face of the column, redistribution to the steel section still allowed sufficient plastic deformations to occur at a fairly high proportion of the peak load.

3.3. Load–deflection

The load–deflection curves for these columns tested as beams are plotted in Fig. 8. Noteworthy is the fact that all columns behaved in a fairly ductile manner with a considerable plastic plateau. Furthermore, premature fracture of the welds was not evident in any of the columns tested.

3.4. Load–strain

The load–strain curves for these columns are useful in determining the onset of yield as well as highlighting local buckling on the compression faces which was inelastic in all the columns and beams tested. A typical load–strain diagram for a column and beam is shown in Fig. 9.

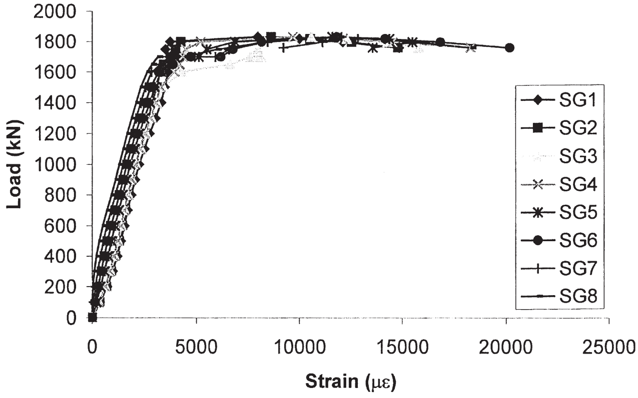

(a) **Column HSS1**

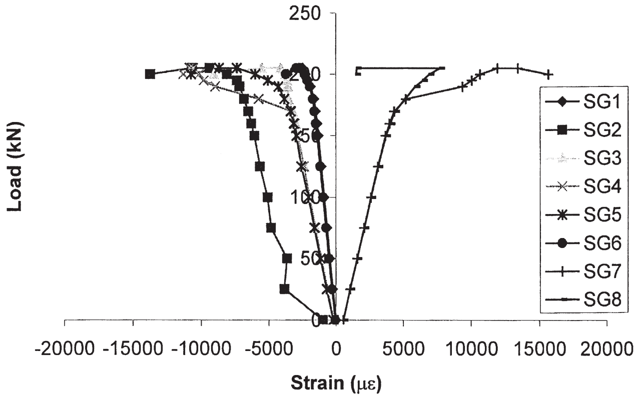

(b) **Beam HSS6**

Fig. 9. Load–strain diagrams.

(a) **Typical Column**

(b) **Typical Beam**

Fig. 10. Failure modes of columns and beams.

Column HSS1 was tested in pure compression and the load–strain response shows that uniform loading was achieved. This figure also shows that the load–strain response was linear up to the peak load of about 1800 kN where compressive yielding began to take place. Some of the strain gauges also show signs of inelastic local buckling, which occurred after significant axial deformation had occurred. Beam HSS6 was tested in pure bending and the load–strain response shows that yielding began in the bottom fibres at an applied load of about 175 kN. After yielding occurred in the bottom fibre, compressive failure of the concrete followed which then promoted some compressive yield and local buckling at the region of failure. However, the strains in the compressive region were not greater than the yield strain when the failure load had been reached.

3.5. Failure modes

The main failure modes associated with these columns included local buckling, concrete crushing, as well as weld fracture. All these failure modes are highlighted in Fig. 10. Local buckling in all specimens was inelastic and concrete crushing generally preceded this. At very large strains, weld fracture occurred as highlighted at the edge of the columns' adjacent plates shown in Fig. 10.

4. Numerical model

A numerical model developed by Uy [8] was augmented with the constitutive relationship for high strength steel. Uy [9] also augmented the model for mild steel thin-walled box columns where local buckling was incorporated in the analysis. Pertinent aspects of this model will be briefly described herein which relate to the implementation of the high strength steel constitutive relationship.

4.1. Method

The numerical model is based on a series of finite slices throughout the depth of the cross-section as shown in Fig. 11. The slices of each cross-section are assumed to develop a strain with respect to an applied curvature, ρ, and the stress–strain relationships of the respective materials are then assigned to that element. Integration of the stress over the area of each slice then allows an axial force to be determined. These forces are then used in the determination of equilibrium of the cross section using Eq. (3)

$$N=\int_A \sigma \, \mathrm{d}A \tag{3}$$

where N is the applied axial force on the cross-section and Eq. (4) then allows the determination of the internal bending moment, M, where

$$M=\int_A y\sigma \, \mathrm{d}A \tag{4}$$

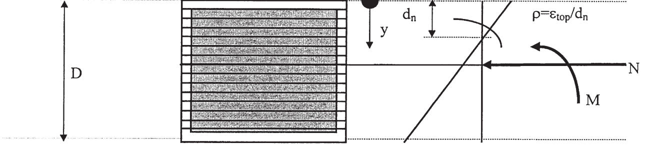

Fig. 11. Method of slices in cross-sectional analysis.

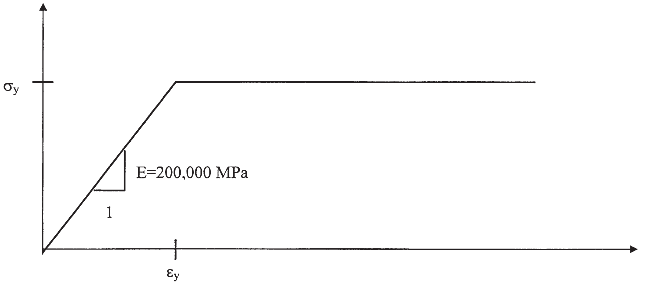

Fig. 12. Idealised stress–strain curve for high strength structural steel.

4.2. Stress–strain relationships

4.2.1. High strength steel

The idealised stress–strain curve for the steel shown in Fig. 12 was used where the yield stress is taken as an average value of 770 MPa based on the average yield stress for the tension and compression tests. This idealisation is due to the difference in stress–strain behaviour determined from both tension and compression tests as illustrated in Figs. 2 and 3. These differences are certain to have been caused through the build up of residual stresses due to the welding process in the compression stub columns.

4.2.2. Residual stresses

The idealised residual stresses are shown in Fig. 4 and these reflect the measured experimental results. These were also incorporated in the analysis by an imposed

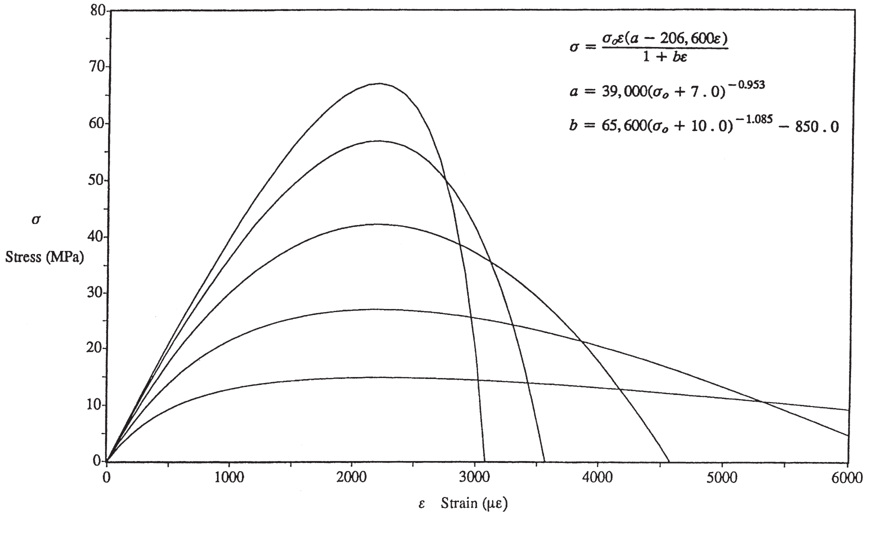

Fig. 13. CEB-FIP (1970) stress–strain model.

residual stress, which was added to the applied loading in each slice. The level of residual stress imposed was dependent on the *b*/*t* ratio and this is outlined in Table 4.

4.2.3. Concrete

The stress–strain law used to model the concrete was that of the CEB-FIP [10] which provides a continuous function of stress with respect to strain and ignores the effect of confinement which is considered negligible in rectangular concrete filled

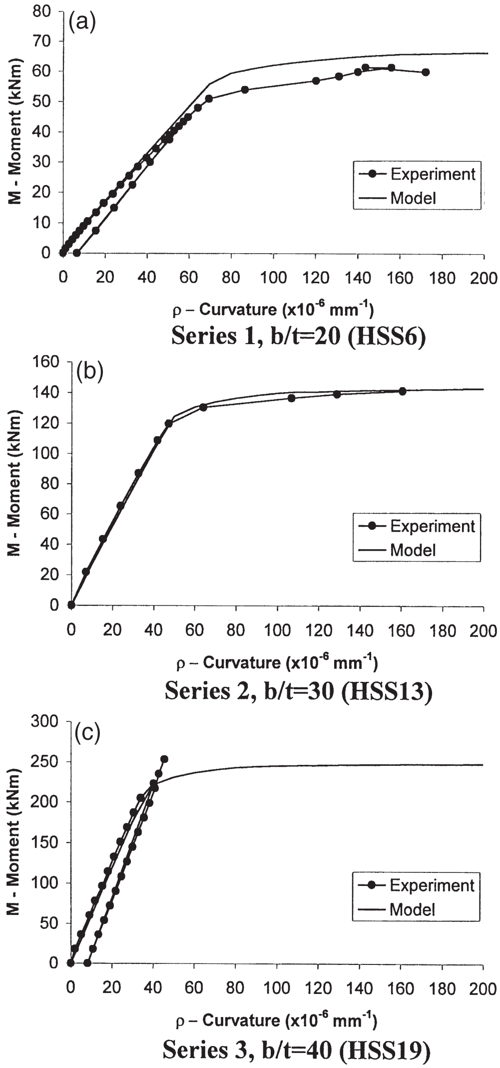

Fig. 14. Calibration of model with experiments.

columns. This stress–strain law is illustrated for various strengths of concrete in Fig. 13.

5. Calibration of numerical model with tests

In order to calibrate the numerical model, the experimental moment–curvature response of each column was compared with that generated from the numerical model. Typical comparisons are shown for specimens HSS6, HSS13 and HSS19 in Fig. 14. This figure shows excellent agreement between experiment and model for the elastic region. Once yielding occurs, the value of peak load is only slightly overestimated by the numerical model in the case of HSS6. For specimen HSS13 an excellent agreement is achieved for both the elastic and plastic range of structural

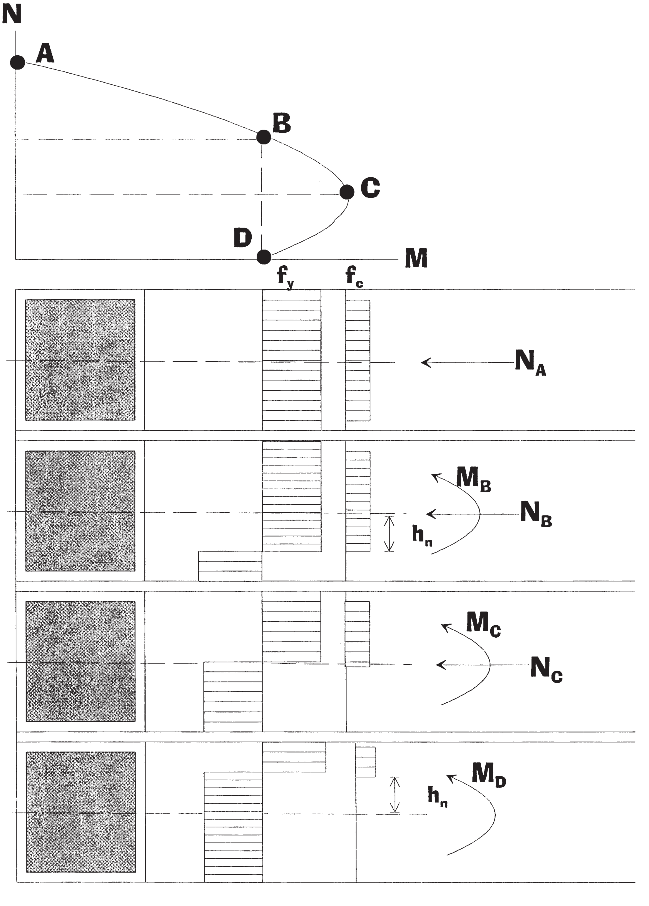

Fig. 15. Eurocode 4 model — rigid plastic.

response. Strains in specimen HSS19 were only measured up to the point of initial yielding and thus a comparison is not able to be obtained in the plastic range. However, the numerical model shows excellent agreement for the elastic range of structural response and the prediction of ultimate moment in the model is slightly less than that achieved in the experiments.

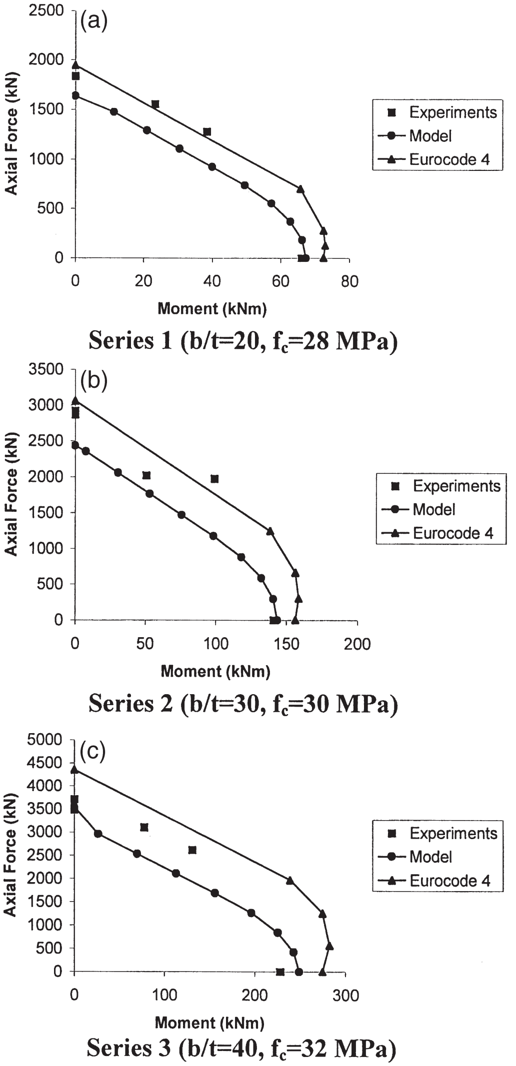

Fig. 16. Comparison of tests, model and Eurocode 4 (rigid plastic).

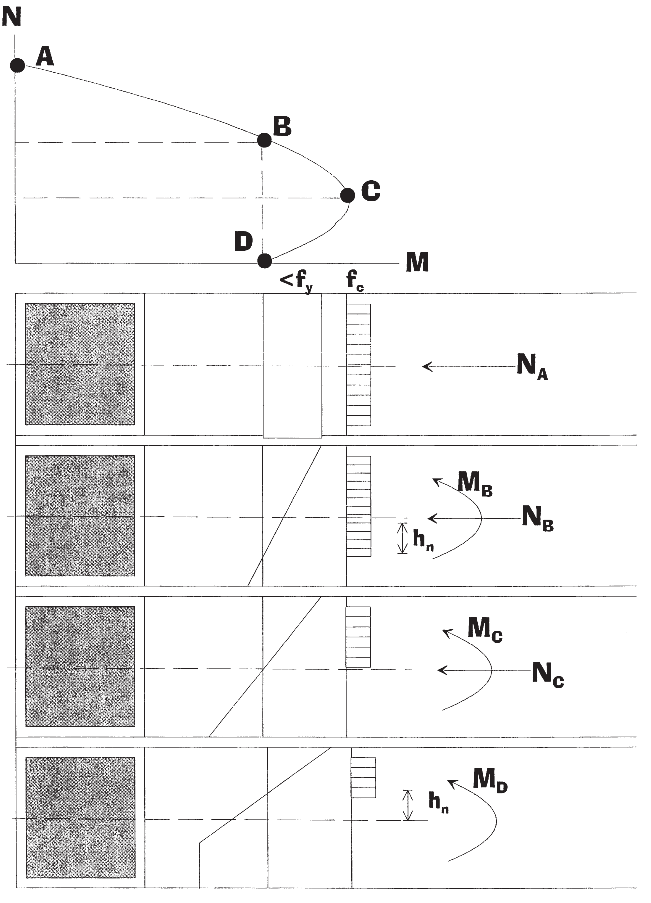

Fig. 17. Modified Eurocode 4 model.

6. Comparison of numerical model and tests with Eurocode 4 — rigid plastic approach

The Eurocode 4 approach allows the construction of the strength interaction diagram by using a rigid plastic analysis approach as shown in Fig. 15. Its simplicity in enabling neutral axis depths, axial forces and bending moments to be determined makes it useful for practising structural engineers. This approach was compared with the numerical model results and the experiments to see if it is applicable for the use of high strength steel. The theoretical model is shown to provide a very good comparison, which is conservative for all the sets of tests as illustrated in Fig. 16. The Eurocode 4 model is, however, found to overestimate the test results as it is based on a rigid plastic analysis, which assumes fully crushed concrete and fully yielded steel. This is particularly true for the points on the interaction diagram for pure compression and pure bending.

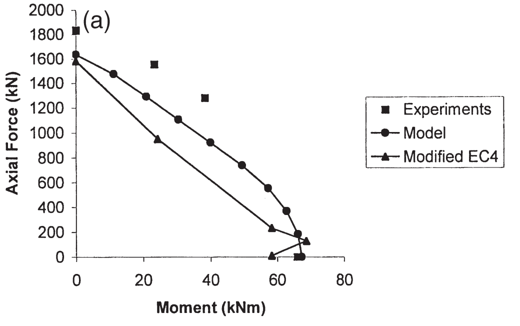

Series 1 (b/t=20, f_c=28 MPa)

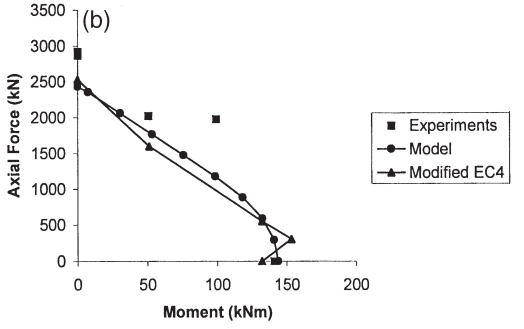

Series 2 (b/t=30, f_c=30 MPa)

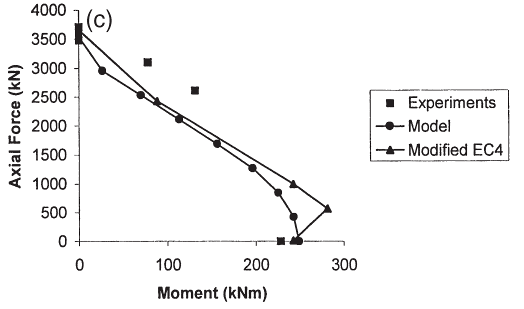

Series 3 (b/t=40, f_c=32 MPa)

Fig. 18. Comparison of tests, model and modified EC4.

Since the EC4 is a design model it may be considered inappropriate in the design of composite columns utilising high strength steel as it is non-conservative in its prediction of strength. In order to develop a design model, which is conservative, a mixed analysis approach was developed.

7. Comparison of numerical model and tests with modified Eurocode 4 — mixed analysis approach

The Eurocode 4 approach was modified by using a mixed analysis approach. This approach assumes the concrete has crushed and the steel is partially elastic, as the strains at the point of crushing of concrete are significantly less than the yield strength of the steel in compression. This approach is illustrated in Fig. 17. For the mixed analysis a greater parity was achieved as shown in Fig. 18 and thus it suggests that it is more applicable for design than the fully rigid plastic model of Eurocode 4. The modified EC4 model is shown to be conservative for all points on the strength interaction diagram for each of the three series considered in the experiments. Thus due to its conservatism this model would be more appropriate than the EC4 model when considering the strength of composite columns utilising high strength steel.

8. Discussion and conclusions

This paper has presented a set of benchmark experiments on the use of high strength steel in composite columns. These tests have then been used to calibrate a numerical model and have been compared with an existing design procedure in Eurocode 4 to consider its applicability for design.

The numerical model was shown to be conservative and fairly accurate in its prediction of the experimental results. However, this model is not amenable for design, as it requires the development of a computer program. The Eurocode 4 approach which is more amenable for design by hand calculation was shown to be unconservative and thus would not be applicable in the design of concrete filled steel columns which incorporate high strength steel. A mixed analysis approach has thus been proposed which assumes the concrete to be plastic and the steel to be elastic and it was shown to produce a conservative but reasonable estimate of the cross-section strength, which is more suitable for design applications.

Acknowledgements

The Australian Research Council supported this project and this is gratefully acknowledged. Furthermore, the author would like to thank Bisalloy Steels, Unanderra for supplying the high strength steel plate for the experiments. This research is part of an ongoing programme at The University of New South Wales on composite steel–concrete structural members.

References

[1] Rasmussen KJR, Hancock GJ. Plate slenderness limits for high strength steel sections. J Construct Steel Res 1992;23:73–96.

[2] Rasmussen KJR, Hancock GJ. Tests of high strength steel columns. J Construct Steel Res 1995;34:27–52.
[3] Uy B, Sloane RJ. Behaviour of high strength steel in composite tee beams. J Construct Steel Res 1998;46(1-3):203–4 (Special Issue: 2nd World Conference on Steel Construction).
[4] Uy B. Local and post-local buckling of concrete filled steel welded box columns. J Construct Steel Res 1998;47(1-2):47–72.
[5] Uy B. Axial compressive strength of steel and composite columns fabricated with high strength steel plate. In: Proceedings of the Second International Conference on Advances in Steel Structures, Hong Kong, 1999. p. 421–8.
[6] Eurocode 4, ENV 1994-1-1 Design of composite steel and concrete structures, Part 1.1. General rules and rules for buildings. British Standards Institution, 1994.
[7] Uy B, Bradford MA. Elastic local buckling of steel plates in composite steel–concrete members. Engng Struct 1996;18(3):193–200.
[8] Uy B. Strength and ductility of fabricated steel-concrete filled box columns. In: Proceedings of the Engineering Foundation Conference on Composite Construction: Composite Construction III, Irsee, Germany, 1996. p. 616–29.
[9] Uy B. Strength of concrete filled steel box columns incorporating local buckling. J Struct Engng, ASCE 2000;126(3):341–52.
[10] Comite Europeen du Beton. Deformability of concrete structures — basic assumptions, bulletin d'information No. 90, 1970.